1965

The effect of mechanical and thermal treatments on the sub-structure of pure copper and a copper alloy dispersed with alumina

Peter R. Bridenbaugh
Lehigh University

THE EFFECT OF MECHANICAL AND THERMAL TREATMENTS ON THE SUB-STRUCTURE OF PURE COPPER AND A COPPER ALLOY DISPERSED WITH ALUMINA

by
Peter R. Bridenbaugh

A THESIS

Presented to the Graduate Faculty

of Lehigh University

in Candidacy for the Degree of

Master of Science

This thesis is accepted and approved in partial fulfillment of the requirements for the degree of Master of Science.

17 Sept 1965
date

George F. Conard
Professor in charge

Head of the Department

ACKNOWLEDGEMENTS

The author would like to thank Professor G.P. Conard II for his encouragement and guidance without which this work could not have been completed. Also, much is owed to Terry Clegg, Timothy Curran, and my wife for their assistance in the preparation of this manuscript and to R.E. Cairns Jr. for suggesting the topic and discussing the results. Finally, the author would like to thank the Carpenter Steel Company for sponsoring the research.

TABLE OF CONTENTS

LIST OF FIGURES

LIST OF TABLES

THE EFFECT OF MECHANICAL AND THERMAL TREATMENTS ON THE SUB-STRUCTURE OF PURE COPPER AND A COPPER ALLOY DISPERSED WITH ALUMINA

by
Peter R. Bridenbaugh

ABSTRACT

The Fourier analysis of the (111), (200), (222) X-ray line profiles obtained by a full proportional counter X-ray diffractometer yielded values for the stored energy, the effective domain size, the lattice strains, the stacking fault probability, and the twin fault probability for pure copper and Cu - 1.1vol% Al_2O_3 deformed by filing.

The domain structure, lattice strains, and stored energy of the pure copper were observed to anneal out at 300°C. On the basis of this information and the stacking fault energy range indicated by the stacking fault probability, a model of the cold worked sub-structure was proposed by Gay et al. It was also concluded that a significant amount of recovery occurred at room temperature.

The sub-structure of the dispersion strengthened copper alloy did not anneal out at the lower temperatures, but underwent recovery until a sub-structure was defined with a domain size of the same order of magnitude as the mean free path between the dispersed particles. The level of the stored energy in this final sub-structure was higher than in the cold worked pure copper indicating the source of the high temperature strength of these alloys. This behavior of the alloy was explained by use of the dual matrix sub-structure model proposed by Rassemusen.

The behavior of these two materials and their respective sub-structure models are discussed and compared with other investigations appearing in the literature.

Introduction

Many of the processes used for the fabrication of metal products involve some degree of cold work so that the investigation of this phenomenon and its effect on the properties and structure of metals and metal alloys has been the subject of much research.

Much of this interest in the effects of cold work on metals is due to the strength increase generally observed in cold worked alloys and the desire to retain this strength at elevated temperatures. Perhaps the most important features of dispersion strengthened metal-metal oxide materials is their stability at higher temperatures.

The early X-ray investigations of cold worked metals were primarily concerned with line broadening and asterism. The broadening observed by these experimenters was attributed to the various following causes:

1. Diffraction broadening due to fragmentation of the metal into crystallites on the order of 10^{-5} to 10^{-6} centimeters. (1,2)

2. Diffraction from crystals of different mean lattice parameters caused by the breaking up of the metal into crystals on the order of 10^{-4} centimeters. (3)

3. Distortion of large crystals on the order of 10^{-4} centimeters. (4,5,6,7,8)

More recent work by a variety of experimenters using more sophisticated equipment has shown that much information about the structure of cold worked metals is revealed by

precise line shapes, small line displacements, and line asymmetries as well as line breadths. (This work is reviewed by Greenough (9) and more recently by Warren (10).). These investigators attribute changes in the forementioned parameters to the following types of structural changes:

1. The formation of small coherently diffracting domains.
2. Lattice strains within these domains.
3. The formation of stacking or deformation faults.
4. The formation of twin or growth faults.

It has been shown that the line broadening is primarily the result of the domain structure and the associated lattice strains, (the fault structures contribute to the broadening in a much smaller amount) whereas the line shifts and line asymmetries result respectively from the deformation and twin faults. This will be discussed in greater detail later.

The most useful information from an X-ray study of a cold worked metal can be obtained from a Fourier analysis of the line profile as reviewed by Warren. (10)

The broadening due to instrumental factors is assumed to be represented by the shape of a peak from an annealed sample. The peak to be analyzed, i.e. the cold worked peak, is a convolution of thetrue broadening (caused by structural changes) and broadening due to instrumental factors.

The shape of these two peaks is then represented by a Fourier series for each peak in terms of a new unit cell of

of orthorhombic axes such that hkl = 001'. Or, in other words, for every reflection hkl from a cubic crystal, it is possible to adopt orthorhombic axes that will make the reflection 00l' which is done only to simplify the mathematical expressions and does not limit this approach in any way.

Then following the method of Stokes (11), the cosine coefficients $H_r(n)$ and the sine coefficients $H_i(n)$ for the cold worked peak are given by

$$H_r(n) = K \sum_{-N/2}^{+N/2} h(t) \cos \frac{2\pi nt}{N} \qquad 1$$

$$H_i(n) = K \sum_{-N/2}^{+N/2} h(t) \sin \frac{2\pi nt}{N} \qquad 2$$

The cosine and sine coefficients for the annealed peaks are given by

$$G_r(n) = K \sum_{-N/2}^{+N/2} g(t) \cos \frac{2\pi nt}{N} \qquad 3$$

$$G_r(n) = K \sum_{-N/2}^{+N/2} g(t) \sin \frac{2\pi nt}{N} \qquad 4$$

The peaks are divided into N equal intervals, (N/2 intervals on either side of the peak maximum), more than large enough to include all of the profile in which there is an observable difference from the background level. This is shown in Figure 1.

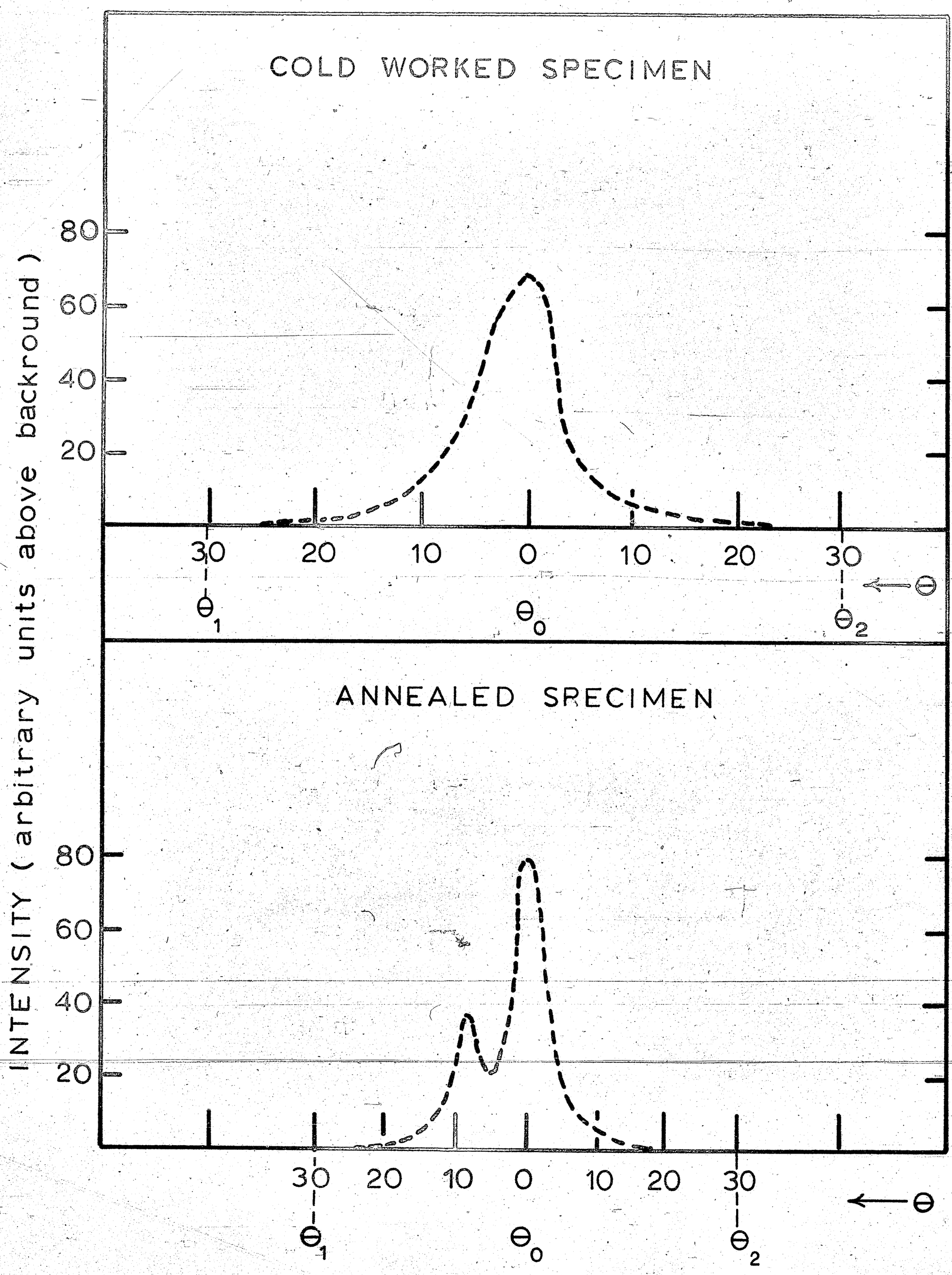

FIGURE 1

SAMPLE DIFFRACTOMETER RECORDINGS FOR PURE COPPER

The functions h(t) and g(t) represent the intensity of the cold worked and annealed peaks respectively as a function of distance along the interval in arbitrary units above the background.

The cosine and sine coefficients of the structural broadened function A_n and B_n respectively , are then given by

$$A_n = \frac{H_r(n)G_r(n) + H_i(n)G_i(n)}{G_r^2(n) + G_i^2(n)} \qquad 5$$

$$B_n = \frac{H_i(n)G_r(n) - H_r(n)G_i(n)}{G_r^2(n) + G_i^2(n)} \qquad 6$$

A unit cell parameter a_3' corresponding to the orthorhombic unit cell giving the 001' reflection is determined for each peak from the point where the tails reach the background. This point is taken as half the distance in reciprocal space from the center of the 001' peak to the next order peak.

$$[(\ell' + \tfrac{1}{2}) - \ell'] = \frac{1}{2} = \frac{2a_3'}{\lambda} (\sin\theta_\perp - \sin\theta_0) \qquad 7$$

Using this interval gives n' harmonic numbers of the Fourier coefficients.

This then designates each coefficient by a length $L = n'a_3'$ which is the true length normal to the diffracting planes. Coefficients are then compared for equal

values L rather than n' as shown in Figure 2 where the cosine coefficients have been normalized after the correction for instrument effects by setting $A_o = 1$.

If the crystal is thought of in terms of coherently diffracting columns of unit cells parallel to the a_3' vector or perpendicular to the diffracting planes (00l'), then the diffracted intensity per unit length of the cone of diffraction from a powder sample, $P'_{2\theta}$, can be written in terms of the corrected coefficients A_n and B_n

$$P'_{2\theta} = K(\theta)\, N \sum_{-\infty}^{+\infty} \{A_n \cos 2\pi n\,(h_3 - 1 - \delta) + B_n \sin 2\pi n\,(h_3 - 1 - \delta)\} \qquad (8)$$

where h_3 is a continuous variable along the 00l' direction in reciprocal space, δ is a peak shift due to one layer (stacking) faults in the normal ABC sequence in fcc structures, (ABCABCBCABC), and N is the average number of units cells in each coherently diffracting domain. In the vicinity of each reflection, $K(\theta)$ is a slowly varying function of θ due to the slow variation of F^2 and $\sin^2\theta$ and is given by:

$$K(\theta) = \frac{\frac{1}{4} M R \lambda^2 F^2}{16\pi\, V_a\, \vec{b}_3\, \sin^2\theta} \qquad (9)$$

where M is the number of crystals in the powder sample, r

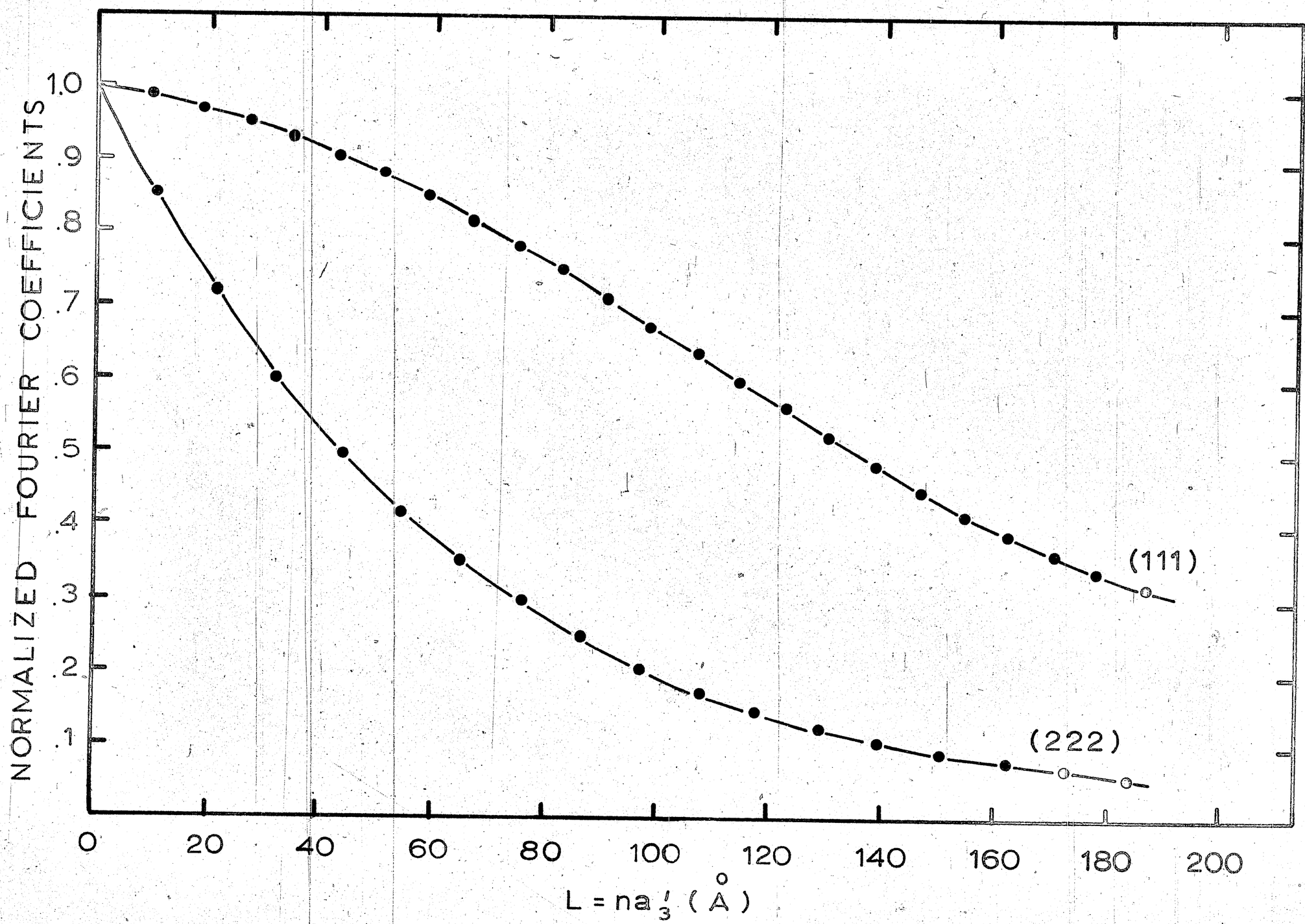

FIGURE 2

FOURIER COSINE COEFFICIENTS FOR COLD WORKED PURE COPPER

is the distance between sample and receiver, V_a is the volume of the unit cell, F is the structure factor, λ is the X-ray radiation wavelength, and $\vec{b}_3$ is a vector in reciprocal space in the 001' direction.

Warren has shown that

$$A_n = \frac{N_n}{N_3} \langle \cos 2\pi \ell n \epsilon_n \rangle \qquad 10$$

$$B_n = \frac{N_n}{N_3} \langle \sin 2\pi \ell n \epsilon_n \rangle \qquad 11$$

where ϵ_n is the strain in a column of n cells, N_n is the average number of cells having an nth neighbor in a given column, and N_3 is the average number of cells in a column normal to the diffracting planes. The brackets signify averages over pairs of nth neighbors in cell columns in the sample, hence an average per column weighted by the number of cells having an nth neighbor in the column. Or, in other words, averaging over all columns of length n in the irradiated sample.

In the cold working of metals, excluding the probability of stacking faults, there is an equal probability of having positive and negative strains so that the sine coefficients B_n are extremely small and can be neglected.

For small values of l and n, the cosine can be expanded to give

$$A_n = \frac{N_n}{N_3}\left[1 - 2\pi^2(h^2 + k^2 + \ell^2)\frac{n^2 a_3'^2}{a_o^2}\langle\epsilon_n^2\rangle\right] \qquad 12$$

where $a_3'(h^2 + k^2 + l^2)^{\frac{1}{2}}/a_o = l$ has been substituted.

The coefficient A_n may be thought of as the product of a particle size coefficient A_n^s and a distortion coefficient A_n^d

$$A_n = A_n^s A_n^d \qquad 13$$

where

$$A_n^s = N_n/N_3 \qquad 14$$

$$A_n^d = [1 - 2\pi^2 h_o^2 L^2 \langle\epsilon_L^2\rangle/a_o^2 \qquad 15$$

where $h_o^2 = h^2 + k^2 + l^2$ and the index n has been replaced by the corresponding length $L = na_3'$.

Thus it is possible to separate the particle size term from the strain for each n by plotting ln A_n versus $h^2 + k^2 + l^2$ using two orders of a line such as 111-222 or 200-400 as in Figure 3. The intercepts at $h_o^2 = 0$ give the particle size coefficients A_n^s which are subsequently plotted against the length $L = na_3'$ to give the particle size. A sample plot is shown in Figure 4. The particle size is determined by using only the first few values of n. Warren (12) justifies this because the Warren-Averbach separation technique is rigorous only for small values of n if the strain distribution is non-Gaussian. This results from the fact that the linear extrapolations made in Figure 3 coincides with the correct

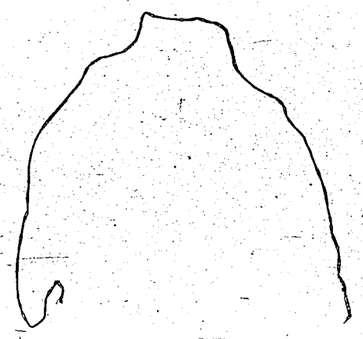

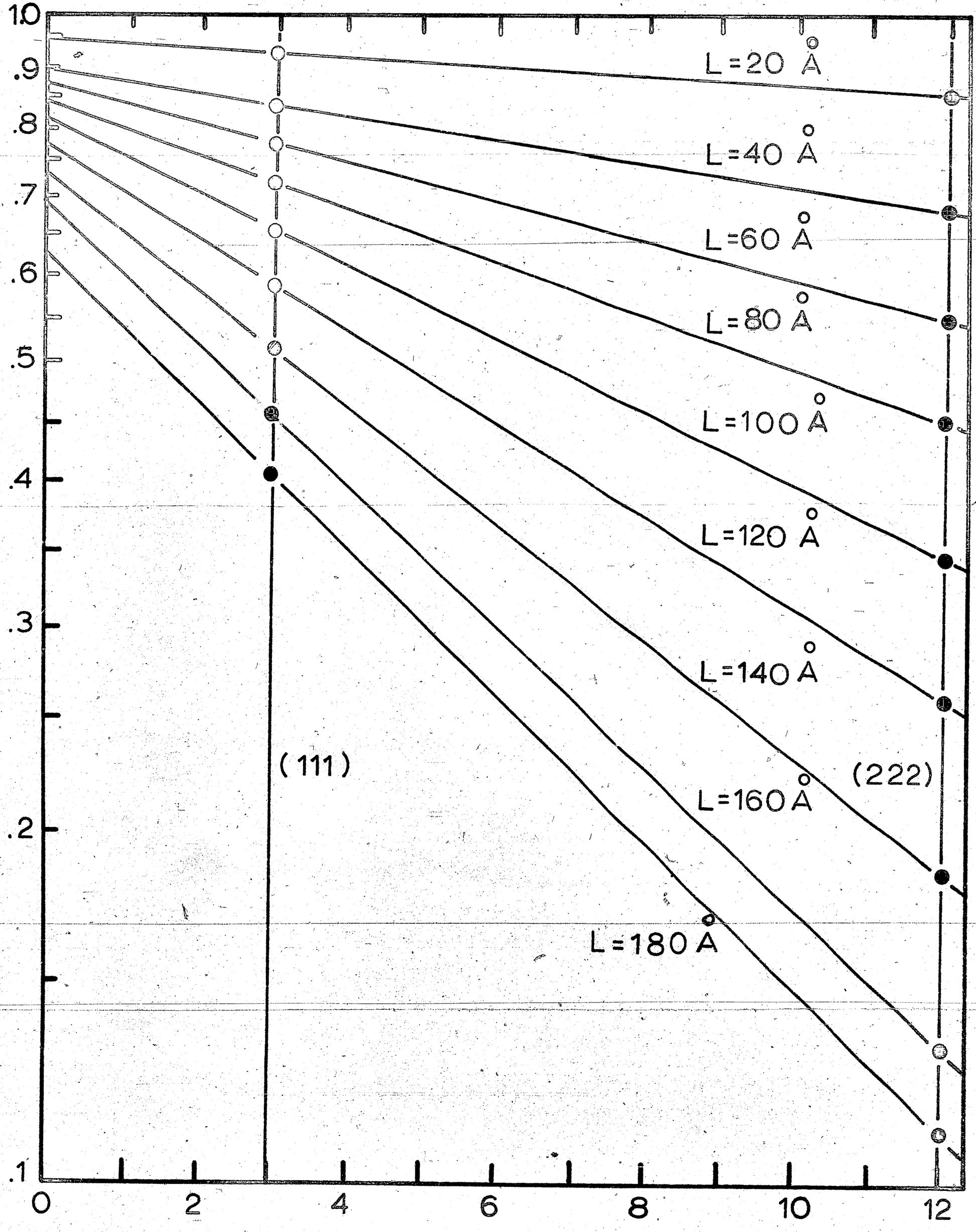

FIGURE 3

LOG A_n vs. h_o^2 FOR COLD-WORKED PURE COPPER

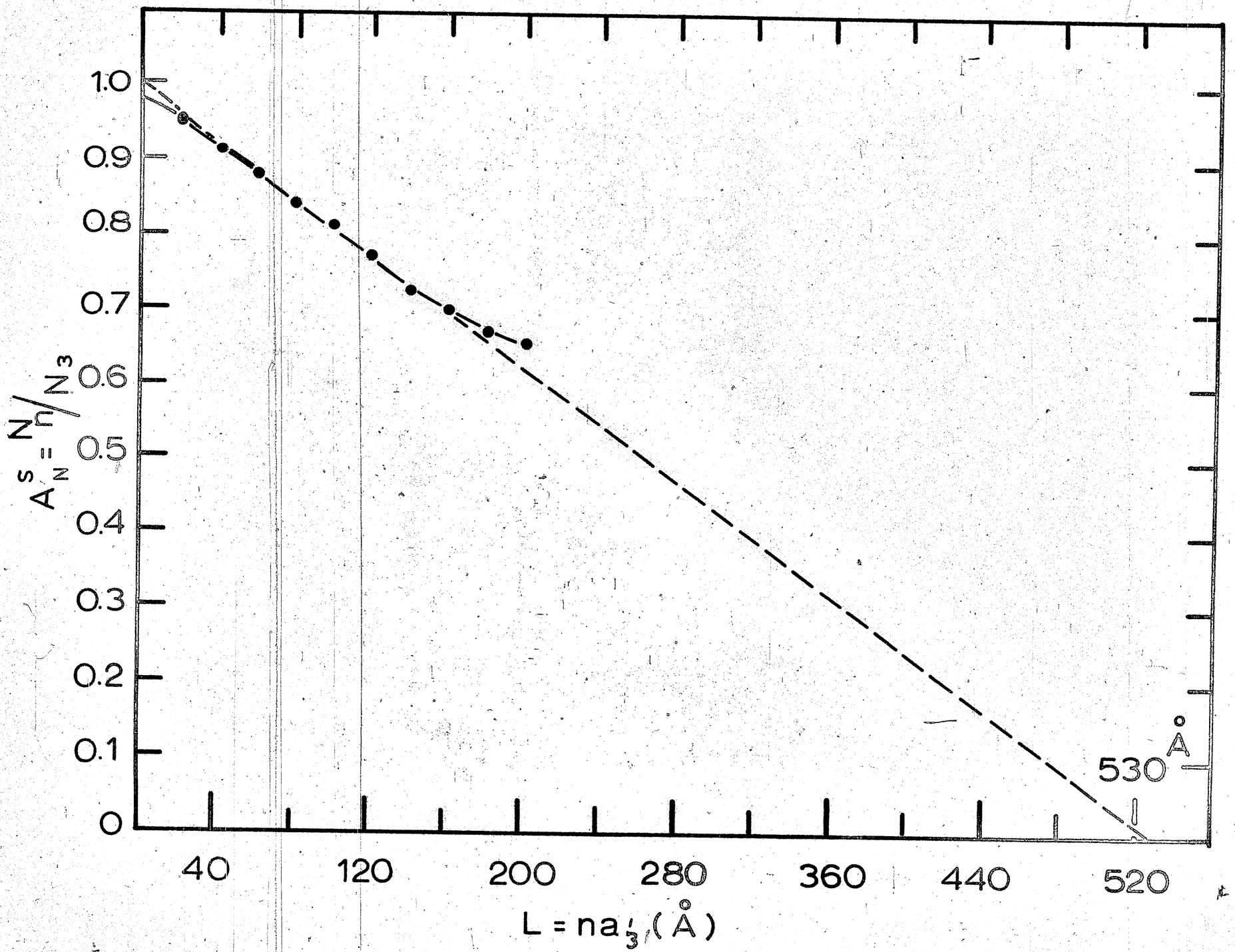

FIGURE 4
PLOT OF PARTICLE SIZE COEFFICIENT EXTRAPOLATED TO GIVE THE AVERAGE PARTICLE SIZE FOR COLD-WORKED COPPER

extrapolations only for those values of the mean square strain that follow a Gaussian distribution.

The initial slope of the ln A_n versus h_o^2 plot gives $2\pi^2 <(\Delta L^2>/a_o^2 = 2\pi^2 L^2 <\epsilon_L^2>/a_o^2$ from which a rms strain $<\epsilon_L^2>$ is obtained.

The rms strain is a strain component normal to the reflecting planes, averaged over the length $L = na_3$, squared, averaged over all regions in the sample, and then raised to the $\frac{1}{2}$ power.

The particle size term Nn/N_3 is related to four quantities: (a) the domain size normal to the diffracting planes, D: (b) the domain size parallel to the diffracting planes, T: (c) the probability of finding a stacking fault between two (111) layers, α, (ABCABCBCABC): (d) the probability of finding a twin or double deformation fault, β, (ABCABCBABCABC) by the following:

$$\left[\frac{d(N_n/N_3)}{dn}<111>\right]_{n \to 0} = \frac{1}{D_{eff<111>}} = \frac{1}{D}$$

$$+ \left(\frac{1.5\alpha + \beta}{a_o}\right)\frac{\sqrt{3}}{4} + \frac{1}{T\sqrt{2}}$$

and

$$\left[\frac{d(N_n/N_3)_{<200>}}{dn}\right]_{n \to 0} = \frac{1}{D_{eff<200>}} = \frac{1}{D}$$

17

$$+ \left(\frac{1.5\alpha + \beta}{a_o}\right) + \frac{1}{T\ 1.5}$$

D and T can be determined by measuring α and β separately and combining Equations (16) and (17). Alternately, minimum values for D or T can be obtained by eliminating α and β in these equations and neglecting the term in T or D.

Stacking faults in FCC structures cause various index lines to shift in different directions whereas general strains cause all lines to shift in the same direction. If stacking faults are present, the 111 line shifts to higher angles and the 200 line shifts to lower angles. This allows the stacking fault probability α to be determined by chart recording continuously from the 111 to the 200 with both the annealed standard and the cold worked sample and then comparing the change in line position as follows

$$\Delta(2\theta^{\circ}_{200} - 2\theta^{\circ}_{111}) = -\frac{45}{\pi}\frac{3\alpha}{2}\left(\tan\theta_{200} + \frac{1}{2}\tan\theta_{111}\right) \quad 18$$

Twin or double deformation faults cause line asymmetries as do general strains; however, strains cause all lines to be asymmetrical in one direction whereas twin faulting causes the 111 to tail to high angles and the 200 to tail to low angles. The twin fault probability, β, can be calculated from the difference in position of the center of gravity and the peak maximum (Δ C.G.). (13)

$$\Delta C G\ (^{\circ}2\theta)_{111} = + 11\beta \tan \theta_{111} \qquad 19$$

$$\Delta C G\ (^{\circ}2\theta)_{200} = - 14.6\beta \tan \theta_{200} \qquad 20$$

However the 111 and the 200 peaks generally overlap if there is much broadening and also, the general strains can cause an asymmetry, so that it is better to evaluate β from an expression of the sum of the above ΔC.G.'s as follows: (14)

$$\Delta C G\ (^{\circ}2\theta)_{111} - \Delta C G\ (^{\circ}2\theta)_{200}$$

$$= \beta(11 \tan \theta_{111} + 14.6 \tan \theta_{200}) \qquad 21$$

This minimizes the difficulties in determining the center of gravity and partially cancels any effects due to general strains. The error in β is less when Equation 21 is used.

If α and β are determined independently using Equations 18 and 21, then Equations 16 and 17 may be used to determine values for the two particle sizes D and T. This,

in general, outlines the experimental technique by which changes in sub-structure can be evaluated.

It is the purpose of this investigation to:

(a) evaluate the effect of cold work on the sub-structure of pure copper and of a dispersion strengthened aluminum oxide-copper alloy by studying the changes produced in the X-ray profile.

(b) evaluate changes in the sub-structure of these alloys produced by various annealing treatments.

(c) determine the role of the dispersoid in these sub-structure changes by comparing the results for pure copper and dispersion strengthened alloy.

(d) evaluate the various mechanisms for dispersion strengthening that have been proposed in the literature.

Experimental Details

The specimens that were used as standards for this investigation were prepared from 99.999% copper rods. The metal-metal oxide system was represented by a Cu - 1.1vol% Al_2O_3 alloy rod. (See Appendix A)

These rods were reduced to powder and cold worked at the same time by filing under ice water. A temperature of 5° C as measured by a standard mercury thermometer was maintained in the bath throughout the filing process. The powders were then put through sieves and only those in the range of minus 200 mesh plus 325 mesh were used in subsequent testing.

The samples for investigating the cold worked state were taken from these powders and the X-ray line profiles were recorded immediately. The remaining powders were sealed in evacuated glass tubes for annealing treatments.

The annealing treatments and the appropriate specimen designation are indicated in Table I. All temperatures were measured with a chromal-alumel thermocouple to an accuracy of $\pm 2^{\circ}$ C. This was verified by a mercury thermometer between 0° C and 200° C. All annealing treatments were for four hours. A thermocouple sealed in a glass tube of copper powder showed that it took five minutes to reach temperature.

The X-ray specimens were prepared by mixing the powders with vaseline and then pressing them into a specially machined Mylar holder. The surface of the powder vaseline

mixture was smoothed by pressing against plate glass.

TABLE I.

ANNEALING TREATMENTS

Powder Used	ANNEALING TEMPERATURE °C				
	50*	100*	300**	400**	500**
Pure Cu	C5	C1	C3	--	C50
Cu-1.1vol%Al_2O_3	CA5	Ca1	CA3	CA4	CA50

* Oil bath
** Electric furnace: Lehigh Met. Dept. Hevi-Duty

A X-ray diffraction pattern of the sample holder filled with vaseline was taken through all angles in 2θ of interest. This showed that there were no diffraction lines, only an amorphous halo at very low angles. These angles were below those of interest so that no interference was anticipated.

The line profiles were obtained using a Siemens full proportional counter X-ray diffractometer with nickel filtered CuK_{a1a2} radiation. A simple diffraction pattern of each sample was made by fast scan at $\frac{1}{2}$ of a degree in 2θ per minute to locate the peak maxima. These were used later for both alignment of the goniometer when necessary and as a basis for selecting the location of the peak maximum in the line profile analysis. The line profiles were taken at a scanning rate of 1/16 of a degree in 2θ per minute for a

minimum of 5^{o} in 2θ on either side of the peak maximum.

Because of the proximity of the (111), (200) peaks, there was a tendency for the tails to overlap. In order to accurately determine the profile of the tail, it was necessary to scan continuously from 5^{o} in 2θ below the (111) peak to 5^{o} in 2θ above the (200) peak. This enabled the exact level of the background to be established.

The line profile was taken graphically from the print out of the diffractometer recorder and coded for a computer program of DeAngelis and Schwartz.[1] (25,26) This program was run on a GE-225 computer and resulted in the calculation of the Fourier coeffeicents and the center of gravity of each line profile. The Stokes (11) method of correcting for instrument broadening was used.

From this information, the particle size, lattice strains, and faulting parameters were calculated for each sample as per the previously discussed technique. A calculation of the stored energy was made based on an expression developed by Faulkner. (27) (See Appendix B)

[1] A Copy of this program can be obtained from the author or from Professor Wayne Kraft, Metallurgy Department, Lehigh University.

Presentation of the results

The effective particle size, the root mean square strain, (averaged over 50 and 100 angstroms), and the faulting parameters appear in Table II. These data result directly from the Fourier analysis of the X-ray line profiles that were taken on the two alloys involved in this investigation in various states of cold work and annealing.

The effect of annealing from the cold worked state on the effective particle size is shown by the plot of domain size versus annealing temperature in Figure 6. The as cold worked domain size of the pure copper is on the order of 250Å and increases rather rapidly with annealing temperature to values that are immeasurable by this technique. This incapability of measurement results from the fact that the domain size of the specimen in question has so closely approached that of the recrystallized standard that the Fourier analysis cannot determine a significant difference between the two. It does not mean that the sub-structure has disappeared or that it is extremely large, but only large relative to the standard specimen.

The Cu-1.1vol%Al_2O_3 alloy has an as cold worked domain size of 325Å, which is slightly higher than that of the pure copper, but not significantly. This fact alone seems to indicate that the cold-worked sub-structure of the two materials is similar; however, as will be shown later, this is not the case. The effect of annealing temperature on the

TABLE II

CALCULATED DATA FROM FOURIER ANALYSIS

SPECIMEN	DOMAIN SIZE Å	RMS STRAIN 50Å %	RMS STRAIN 100Å %	STACK. FAULT PROB.	TWIN FAULT PROB.
CCW	275	0.14	0.115	0.0028	0.004
C5	550	0.098	0.063	----	----
C1	925	0.07	0.042	----	----
C3	---	0.025	0.018	----	----
CACW	325	0.275	0.225	----	----
CA5	425	0.19	0.14	----	----
CA1	525	0.16	0.12	----	----
CA3	1100	0.10	0.06	----	----
CA4	1300	0.09	0.05	----	----
CACW*	350	0.600	0.527	----	----
CA5*	750	0.42	0.353	----	----
CA1*	1000	0.27	0.170	----	----
CA3*	3400	0.21	0.130	----	----
CA4*	4025	0.19	0.116	----	----
CA50*	4200	0.18	0.110	----	----

* Standard C50

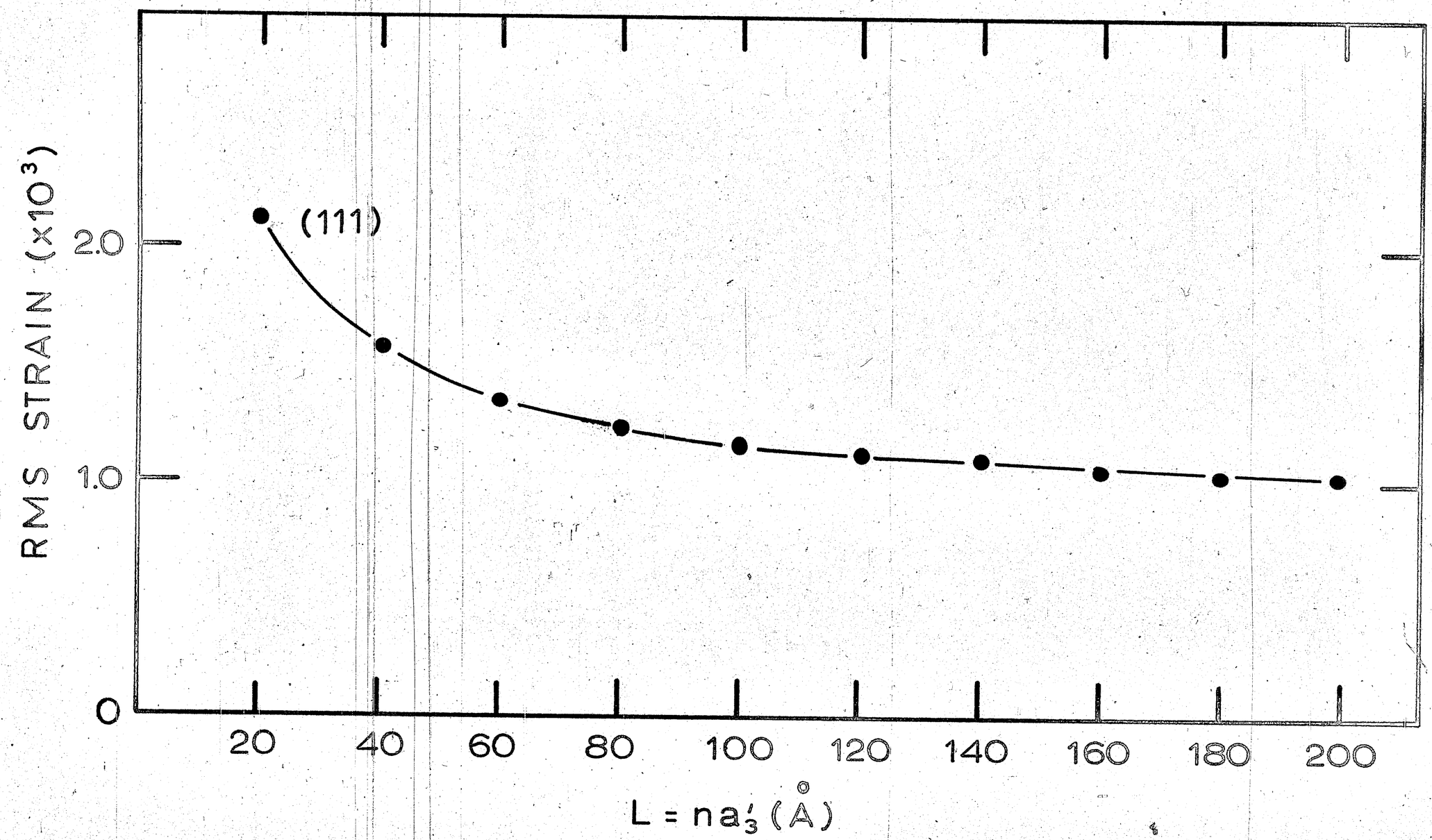

FIGURE 5

STRAIN DISTRIBUTION FOR COLD WORKED COPPER

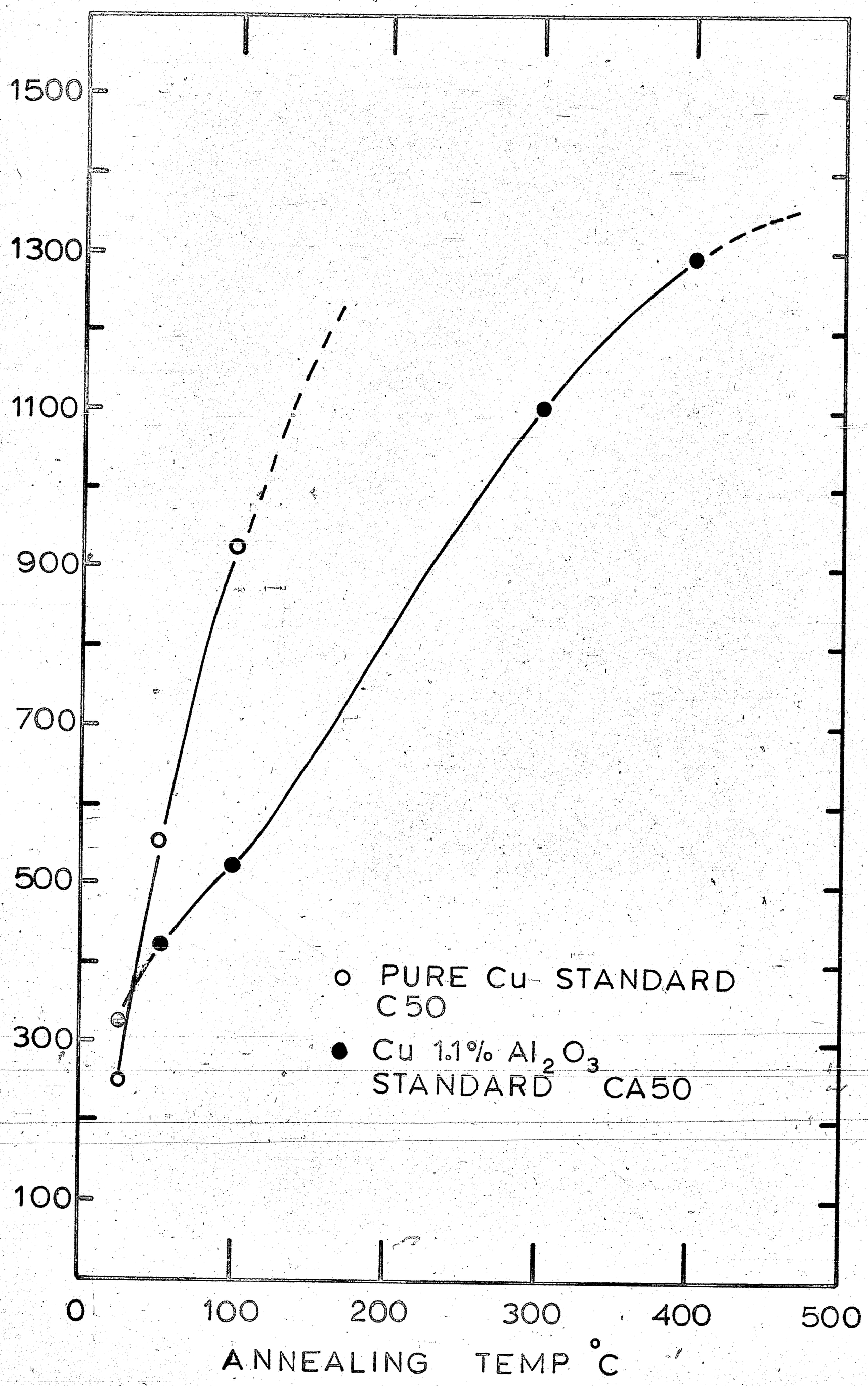

FIGURE 6

DOMAIN SIZE AS A FUNCTION OF ANNEALING TEMPERATURE

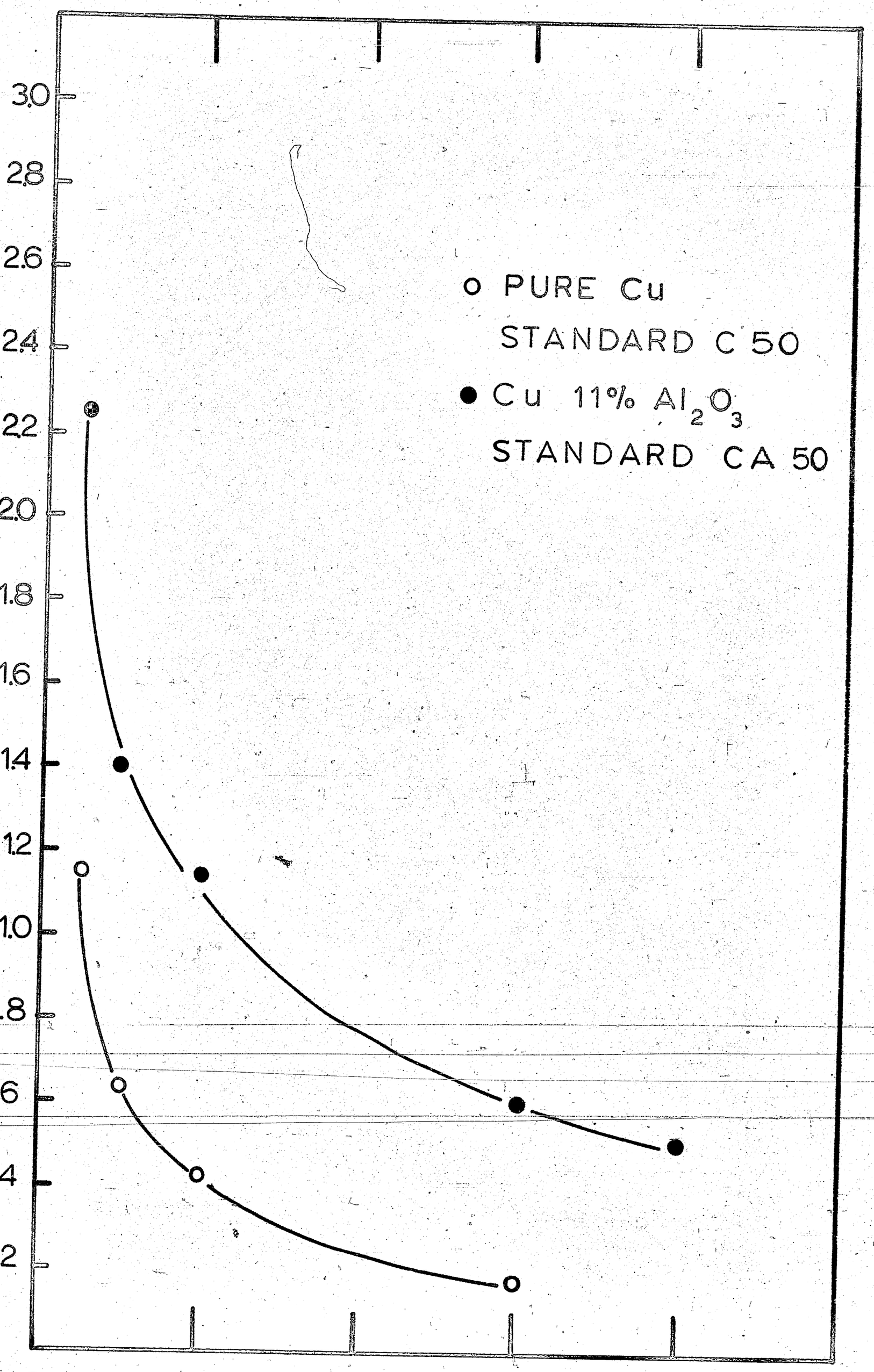

FIGURE 7

RMS STRAIN AS A FUNCTION OF ANNEALING TEMPERATURE

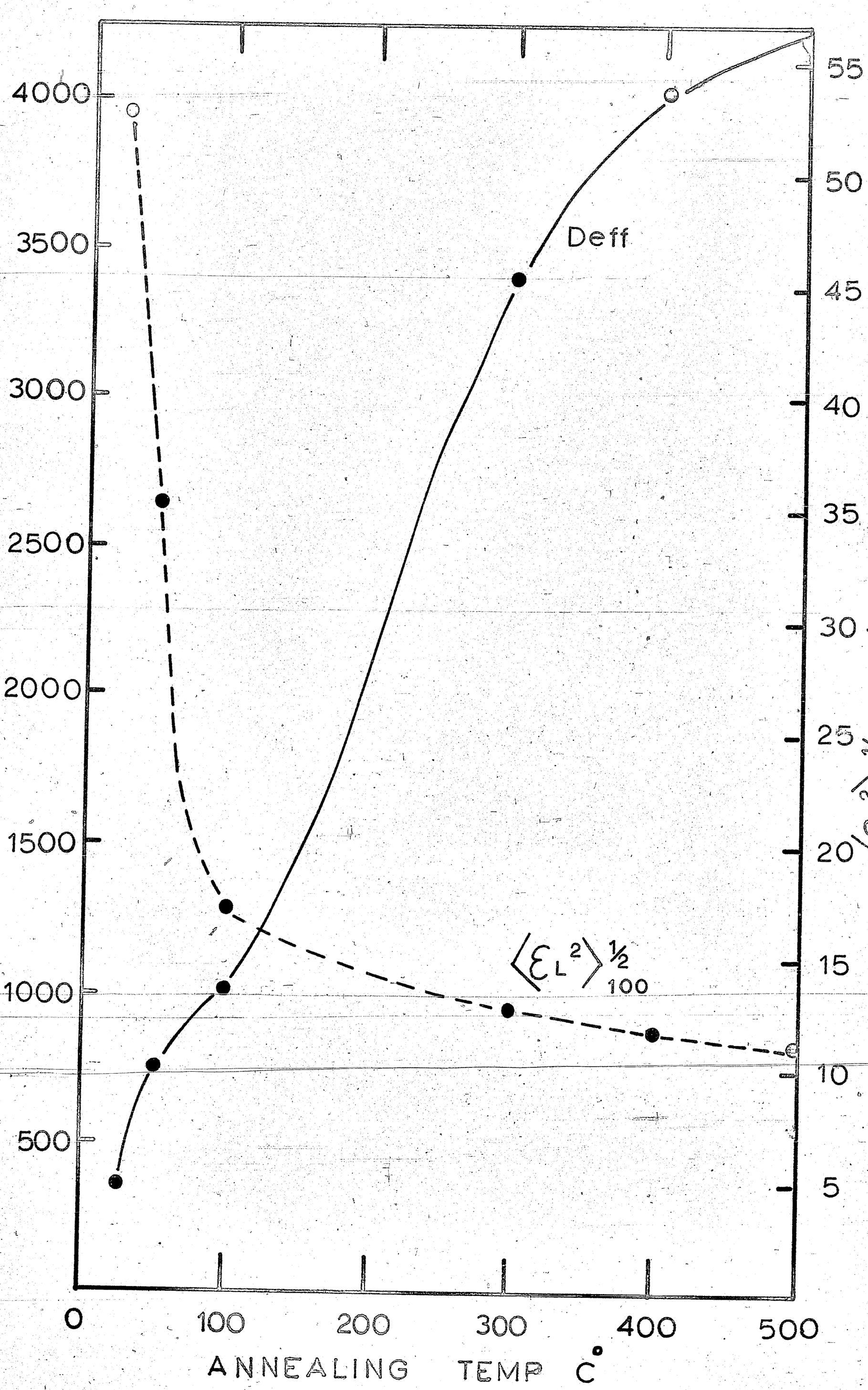

FIGURE 8

DOMAIN SIZE AND RMS STRAIN FOR Cu-1.1% Al_2O_3
DETERMINED WITH PURE COPPER STANDARD: C50

dispersion strengthened alloy is much less than this effect on pure copper. Also the domain size appears to level off at the higher temperatures. The recrystallization temperature of this alloy for a four hour anneal is on the order of 1050°C, (16,28), so that the standard CA50 (which was annealed at 500°C) is not recrystallized. The data in Figure 6, while not giving a true picture of the substructure in the CA alloy series, are still useful in evaluating substructure changes. In order to offset the strains in the standard CA50, the data for the CA alloy series were re-evaluated using specimen C50 as a standard. These data are included in Table II and are plotted in Figure 8. Again the as cold worked domain size is around 350Å and increases with annealing temperature to a value of 4200Å at 500°C where it appears to be leveling off. This is the same order of magnitude as the mean free path in the matrix of the dispersion hardened alloy.

The root mean square strain averaged over 100Å is shown in Figure 7 for both materials as a function of annealing temperature. The as cold worked pure copper has a rms strain of about 0.11% whereas the CA alloy has a rms strain of 0.22% based on standard Ca50 or about 0.53% based on standard C50. In either case, there is a considerably larger strain in the CA alloy lattice. Upon annealing, the pure copper showed a decrease in strain to 0.18% at 300°C. A

pure copper powder annealed at 400°C showed no strains that were large enough to detect by this method to any degree of acccuracy. These values are of the same order of magnitude as the values obtained for pure copper by Agnihotri and Mitra. (29)

The annealing behavior of the CA alloy with the CA50 standard was much the same as for the pure copper. The strain dropped off to a level of 0.05% at 400°C or about two and one half times that for the pure copper. The CA alloy retained about 25% of its initial cold worked strain at the 400°C level. There is a noticable trend for this decrease to level off. The more interesting information comes from the comparison with the C50 standard, Figure 8. The retained strain is again about 25%, but leveling off is much more pronounced and is extended to 500°C, which indicates that this leveling off is real. The strain at these higher temperatures is greater than that in pure copper by an order of magnitude.

The change in the rms strain averaged over 50Å was similar as can be seen in Table II. The significance of the averaging over various distances can be seen in Figure 5. This is a typical strain distribution obtained from a line profile analysis. There are two interesting features of this curve. The first is the leveling off of the strain values at the larger averaging distances. This can be attributed to the inhomogeneity in the strains and the fact that at the

larger distances the smaller domains which contain the highest strains no longer contribute. (10) The second feature is the increasing strain with decreasing L to the point where the slope appears to approach infinity so that extrapolation to L = 0 is difficult if not impossible to do with even reasonable accuracy. The significance of these high strains at small distances is that they indicate that the structure faults or the lattice perturbations that are the source of them are dislocations. Another way of looking at this is that strains must vary with distance from an imperfection so that if the imperfection is of atomic size such as a dislocation, the presence of a strain variation over atomic dimensions indicates the presence of such imperfections.

The stacking fault probability measured for pure copper in this investigation is very low. The value of 0.0028 is on the same order as that observed by other investigators. (29,32) However all these investigations including the authors were made at room temperature where there is known to be appreciable recovery. (30,31,32) Wagner (31) measured the stacking fault probability at -160°C and then allowed the specimens to anneal at room temperature and remeasured the stacking fault probability and found that most of the faults had annealed out.

The value obtained for the twin fault probability of the pure copper was 0.004 which is of the same order of magnitude that has been observed by other investigators. Both

stacking faults and twin faults were seen to anneal out at 50°C as would be expected after the noticable amount of recovery at room temperature.

No values for these faulting probabilities were obtained for the dispersion strengthened alloy. It is believed that the effects of faulting on the line profile were masked by the domain size and lattice strain broadening and also the peak shifts due to general strains.

The low values of the stacking fault probability are indicative of two things. The first is the ability of copper or even the copper matrix of the dispersion strengthened alloy to undergo significant recovery at room temperatures. The second is the presence of a high stacking fault energy which is necessary for cross- slip of dislocations and the formation of a mosaic type sub-structure.

The results of the stored energy calculations appear in Table III. These calculations were based on the mean square strain at 100 angstroms.

The stored energy in the pure copper in the cold worked condition is lower than that measured by other investigators, (29,33), but is not off by an order of magnitude. This suggests that a considerable amount of recovery has taken place at room temperature as has been suggested previously. The initial stored energy of cold work of the CA alloy is much higher as would be expected from the higher strains. The stored energy of both materials drops off rapidly and then

levels out with the CA alloy retaining a greater portion of the initial cold work. This effect is even greater in the CA alloy data calculated using the recrystallized standard C50. This type behavior, when accompanied by the increasing domain size, suggests that the smaller domains release their energy much more rapidly than the large domains which, in the CA alloys, appear to be quite stable.

The observed large decrease in stored energy during the recovery process is of the same order of magnitude as that of Williams (33) who found that at least 50% of the stored energy in cold worked solid copper was released during recovery.

TABLE III

SPECIMEN	STORED ENERGY (cal/gm)	SPECIMEN	STORED ENERGY (cal/gm)
C-CW	0.012	CACW	0.062* 0.34**
C5	0.0035	CA5	0.024 0.15
C1	0.0016	CA1	0.016 0.035
C3	0.0003	CA3	0.0044 0.0193
		CA4	0.0031 0.0164
		CA5	------ 0.0155

*Standard: CA50 **Standard: C50

Discussion of the Results

The behavior of the pure copper can be readily explained in light of the information obtained from this investigation. Filing is one of the most severe deformation processes resulting, therefore, in a high state of residual stress in the metal. Because of this deformation, the slip planes rapidly become saturated with dislocations, cross-slip occurs and a three dimensional network of dislocations is produced in the form of a cellular structure or mosaic pattern. This model of a cold worked structure consisting of small sub-grains of relatively perfect lattice with a low dislocation density separated by regions of heavily distorted lattice with a high dislocation density was the result of microbeam X-ray studies by Gay et al (34). However, the formation of this cellular structure depends upon the ability of the dislocations in the material to cross-slip which in turn is dependent upon the stacking fault energy of the material among other things. A low stacking fault energy produces wide faults separating partial dislocations. Obviously, these extended dislocations would have difficulty transferring from one slip plane to another except at points where the two partials come together. On the other hand, a high stacking fault energy would allow fewer faults to be produced and those that did exist would be extremely narrow allowing cross-slip to occur much more easily.

The low stacking fault probability observed from this material indicated a relatively high stacking energy. The

stacking fault energy of copper given by Van Bueran (36) is 160 ergs/cm^2 which makes it one of the higher energies. (Al, Ni, Ag, 238, 300, 29 ergs/cm^2 respectively). Thus it is safe to conclude that the stacking fault energy in copper is high enough to allow cross-slip to occur easily and form the proposed cellular structure. However, since this energy is not extremely high, some impeding of cross-slip would be expected resulting in a higher dislocation density in the sub-grains and a lower dislocation density in the boundary regions than experienced in other materials, nickel, for instance. If this were the case, the lower temperature annealing treatments would have a greater effect and domain structure as well as the strains would begin to anneal out with these treatments. This was observed to occur for the pure copper in this investigation.

Mitchell and Haig, (35), working with nickel (SFE = 300 ergs/cm^2) found that the lower temperature anneals relieved the strain in the less heavily deformed regions and did not cause an increase in domain size and thus concluded that the model of Gay et al applied. With this in mind, the proposal that was made for copper that because of the lower stacking fault energy there is a lower dislocation density in the boundaries and a higher dislocation density in the sub-grains than in other cold worked materials seems to be valid. This is in reality only a modification of the Gay model.

Considering this model for the cold worked structure,

the effect of the annealing treatments on the structure may be explained. The low temperature anneal (50°C) provides the thermal activation necessary to allow some of the dislocations in the tangles to glide. This results in a redistribution of dislocations on the slip planes and a slight decrease in dislocation density due to annihilation of dislocations of opposite sign. The result of this is to allow the domain size to increase and the lattice strains to decrease.

This behavior is explained by the proposed model because the lower dislocation density in the sub-grain boundaries makes it easier for the sub-grain to grow and also, the higher dislocation density in the sub-grain itself contributes to the lattice strains and it is these strains in the less heavily deformed regions that anneal out first.

Enough recovery has taken place at the low temperature anneal as evidenced by the decrease in stored energy so that the 100°C anneal provides enough thermal activation to greatly increase the mobility of the dislocations. The dislocations are then redistributed and their density is decreased by the processes of glide and climb. Hence there is a much larger decrease in strain and increase in domain size.

The annealing treatment at 300°C is then enough to cause recrystallization of filings.

The proposed model or modification of the Gay model is thus seen to account for all the observed aspects of the behavior of the pure copper.

The behavior of the dispersion strengthened alloy is markedly different from that of pure copper and hence requires a different model.

The as cold worked strains and stored energy values are considerably higher and the effect of the annealing treatments is much less. Therefore, both the role of the dispersoid in the deformation process leading to the cold worked structure and the role of the dispersoid in the annealing process must be considered and incorporated into the model. However, part of the difference in the as cold worked structures that were observed must be attributed to the effect of the dispersoid on the room temperature recovery process so that the structures are dependent upon both roles.

The obvious role of the dispersoid in the deformation process is that these particles act as obstacles to the movement of the dislocations. Mott and Nabarro (18) made one of the first analyses of this problem and proposed that the moving dislocation line would be in the form of a smooth curve rather than a straight line. Then one portion of the dislocation line can move independently of another portion so that random interactions of the dislocations with the particles do not cancel out. The particles would require the dislocation line to bend around them, at least until they could cut through the obstacle, which would increase the length of the dislocation line and hence require the expenditure of extra energy. Orowan (19) proposed that the yield stress was

inversely proportional to interparticle spacing because that stress was determined by the shear stress necessary to extrude the dislocation line between two particles. The passing of the dislocation line between the particles leaves them encircled by a small dislocation loop. Each succeeding dislocation passing between the particles would add another loop. As the number of loops build up, the interaction with the moving dislocation line is greater and it becomes harder and harder for the dislocation to break away from the pinning action of the particle. The yield point occurs when the stress is high enough to cause a large number of dislocation to break away from the particles and multiply by the double cross-slip mechanism of Orowan. As the deformation continues, cross-slip occurs allowing dislocations to eliminate long range stresses and in doing so form sub-grain boundaries of tangled dislocations pinned by the particles.

This basic model of the deformation process has been substantiated by several investigators, although there is some variation in the mathematical expressions derived from the data. (15, 16, 17, 20, 21, 37)

The major role of the dispersoid in the annealing process seems to be that of retaining the cold worked structure. Preston and Grant (15) first suggested that the retention of strain energy from the deformation in the extrusion operation was the cause of the strength of dispersion strengthened alloys.

It was proposed by Averbach et al (38) that most of the stored energy in a cold worked metal can be attributed to the presence of sub-grain boundaries. Preston and Grant (16) then proposed that the dispersoid pinned the sub-grain boundaries thus retaining the stored energy of cold work in a manner similar to that observed by Zener (39) for grain boundaries. In addition to their own data, the data of earlier investigators Hyam and Nutting (40) and Northcott (41) was interpreted as substantiating this model.

This model however, cannot account for the large increase in particle size that was observed upon annealing at low temperatures and the subsequent leveling off of this growth.

This behavior can in part best be explained by the dual matrix model proposed by Rassemusen (24) for nickel dispersed with thoria. This model separates the metal into two matrices, one matrix composed of the dispersoid particle and the alloy immediately surrounding it and a second matrix composed of the alloy in between the dispersoid particles. For the alloy in this investigation, the matrix A will include the Al_2O_3 particle and the immediately surrounding copper and the matrix B will include the remaining copper. The as cold worked structure described by this model consists of a three dimensional dislocation network some branches of which are locked by the dispersoid, and a large more or less independent tangle of dislocations in the material immediately sur-

rounding the dispersoid (matrix A). The main matrix, (matrix B) in between the dispersoid particles behaves in the same manner as the non-dispersion strengthened during annealing treatments. Matrix A however, behaves in a different manner being much less effected by the annealing treatments.

The lower temperature anneals cause the dislocations in matrix B to glide and climb as in pure copper resulting in a decrease in lattice strain, a decrease in the dislocation density, and an increase in the domain size. This increase in domain size occurs by the migration of the sub-grain boundaries (or branches of the dislocation network) that are not pinned by the dispersoid. The structure at this point consists of a mosaic pattern of sub-grains with some of the boundaries being the dislocation networks that connect the dispersoid particles and are thus pinned by them, and the remaining boundaries being dislocations networks pinned at one end only or not pinned at all. It is the latter boundaries that migrate at the lower annealing temperatures. As the annealing temperature increases, these non-pinned boundaries undergo a decrease in dislocation density and then migrate so that the domain size increases. This process continues until a sub-structure is established consisting of sub-grains that are defined by those boundaries that are pinned.

However, matrix A has not undergone this change. Dislocation climb in this matrix is much more difficult due to the increase in climb distance added by the dispersoid so

that the degree of annihilation of opposite signed dislocations is much less and hence the dislocation density does not decrease much. This will leave each Al_2O_3 particle surrounded by a ring of tangled dislocations that is so stable that it will remain even after the sub-grain boundaries have become unpinned. It is the existence of this structure that accounts for the high amount of stored energy remaining in dispersion strengthened metals even at high temperatures.

This explanation of the observed behavior of the Cu-Al_2O_3 alloy based on the existence of two different matrices appears even more valid when it is noted that the observed domain size at which the growth leveled out is of the same order of magnitude as the mean free path of the alloy.

The final proof of this model lies in the explanation of the changes in the peak shape during annealing. It was observed that the broadening in the tails decreased only slightly, most of the changes in line profile occurring in the center portion even at the higher temperature. The tails of the peak represent the most heavily distorted regions in the crystal and result mostly from the strains in these regions. It could be concluded then that these heavily deformed regions correspond to the sub-grain boundaries. However, since the stored energy and strains in the annealed CA alloy are higher than in the cold worked pure copper structure, it is obvious that the boundaries alone cannot account for all

of the broadening in the tails. This additional broadening and hence the stored energy and strains can then be attributed to the proposed matrix A with the high dislocation density.

Conclusions

1. While the stacking fault energy of the pure copper is high enough to allow cross-slip to occur rather easily, it is not high enough to allow cross-slip to occur to the extent necessary to produce the clearly defined sub-structure proposed by Gay et al.

2. A modified Gay model has been proposed that accounts for the behavior of this less clearly defined sub-structure. This model has a higher dislocation density in the sub-grain and a lower dislocation density in the sub-boundary than the Gay model. This structure is affected to a greater degree by low temperature annealing treatments so that it is readily annealed out.

3. The structure and the annealing behavior of the Cu-1.1% Al_2O_3 alloy is much different that that observed for the pure copper so that another model is needed. A model based on the dual matrix theory of Rassemusen was proposed to account for the behavior of this alloy.

4. The dispersed phase appears to lock some of the sub-grain boundaries in place and thus define a sub-structure with a domain size of the same order of magnitude as the inter-particle spacing after annealing at 500°C.

5. The stored energy present in annealed structure is concluded to result from a high dislocation density surrounding the dispersoid particles.

APPENDIX A

PREPARATION OF Cu Al_2O_3 ALLOY BY INTERNAL OXIDATION.

The starting material was a Cu - 0.23wt%Al alloy in the form of vacuum-melted, chill cast rods one inch in diameter and eight inches long. These bars were reduced 50% by cold swaging and then homogenized at 1000°C for 50 hours in helium.

The homogenized bars were reduced to chips by a milling machine and further reduced in a stainless steel rod mill for four hours. Only those particles passing through a 20 mesh screen were used for the internal oxidation process.

A 450 gram sample of this alloy powder was surface oxidized to cuprous oxide (plus solute oxide) by heating in a measured volume of oxygen at 450°C. The powder was then sealed in a 1.5 inch diameter copper tube and heated to a temperature of 750°C for the internal oxidation process. This allowed the oxygen from the surface oxide to diffuse into the sample.

This powder was then reduced in hydrogen at 450°C for one hour and packed by vibration to a pack density of 50% in a copper container 1.4 inches I.D. and 4.5 inches long. This container was evacuated and sealed for extrusion. This material was extruded at 760°C at a ram speed of 55 ipm and an extrusion ratio of 28 to 1. The final diameter of the alloy rod was 0.25 inches.

This treatment resulted in an internally oxidized Cu alloy containing 1.1 vol% Al_2O_3. The average particle radius was 60 angstroms and the mean free path in the matrix was 0.72 microns.

APPENDIX B

STORED ENERGY CALCULATION FROM X-RAY LINE PROFILE

The stress at any point in a crystal may be described by the direction of the principal stress axes (x',y',z') and the magnitude of the principal stresses ($f_{x'x'}$, $f_{y'y'}$, $f_{z'z'}$). The principal axes (x',y',z') are chosen so as to make $e_{x'y'} = e_{y'z'} = e_{z'x'} = 0$. Then, the principal strains are given by equations of the following form

$$e_{z'z'} = (f_{z'z'} - vf_{x'x'} - vf_{y'y'})/E \qquad (1)$$

where E is Young modulus and v is Poisson's ratio. Equation (1) is Hooke's law in three dimensions and hence only applies in the elastic region.

A mean square principal stress, f^2, and a stress correlation constant, C, may be defined as follows

$$f^2_{x'x'} + f^2_{y'y'} + f^2_{z'z'} = 3f^2$$

$$f_{x'x'}f_{y'y'} + f_{y'y'}f_{z'z'} + f_{z'z'}f_{x'x'} = 3Cf^2 \qquad (2)$$

From the line profile analysis, the mean square variation in the separation of the lattice planes, (da/a), causing the reflection, may be obtained. This mean square variation is equal to the strain component acting along the normal to the reflecting planes. If z'' designates the normal axis and if (l,m,n) are the direction cosines of the z'' axis relative to the principal axes, then the mean square value of the variation in lattice spacing, (alternatively, the mean square value of the strain $e_{z''z''}$) over all parts

of the crystal is given by

$$e^2_{z''z''} = (n^2 e_{z'z'} + l^2 e_{x'x'} + m^2 e_{y'y'})^2 \qquad (3)$$

Now assume that there is an isotropic stress, strain distribution over the entire crystal or that the principal axes are isotropically distributed and further assume no correlation between the magnitude of the principal stresses and their direction cosines. Then from equations 1,2,and 3

$$(da/a)^2 = f^2/5E^2(3-4v + 8v^2 + 2C(1-8v + 6v^2)) \qquad (4)$$

The stored energy is

$$V = \tfrac{1}{2}(f_{x'x'}e_{x'x'} + f_{y'y'}e_{y'y'} + f_{z'z'}e_{z'z'}) \qquad (5)$$

or $V = 3f^2(1 - 2Cv)/2E$

Now, the stored energy may be expressed in terms of the mean square separation of the lattice planes by

$$V = \frac{15E}{2} \frac{(1-2Cv)(da/a)^2}{3-4v + 8v^2 + 2C(1-8v + 6v^2)} \qquad (6)$$

To evaluate the constant C, it is necessary to make some assumptions about the strain distribution in the crystal.

One assumption is that the three principal stress components are independently distributed so that the mean value of the $f_{x'x'}$ $f_{y'y'}$ type products is zero. This corresponds to C = 0 then, if v = 1/3

$$V = \frac{15E\ (da/a)^2}{2(3-4v + 8v^2)} = 2.93\ (da/a)^2 \qquad (7)$$

A second assumption is that only shear stresses are present in the crystal so that the hydrostatic components

are zero. This is equivalent to $C = -\frac{1}{2}$ and equation 6 becomes

$$V = \frac{15E(da/a)^2}{4(1 + v)} = 2.81E\ (da/a)^2 \qquad (8)$$

Equation 8 with its assumption of only shear stresses is probably the more realistic with respect to the strain field of an isolated dislocation in an isotropic material. However, the numerical difference between the two equations is very slight.

The stored energy calculations for this investigation were made using equation 8 and the following constants

Constant	Pure Cu	Cu- 1.1vol% Al_2O_3
Young's Mod.	17×10^6 psi	23×10^6 psi
Density	8.96 gm/cm^3	8.75 gm/cm^3
Poissons Rat.	0.33	0.33

BIBLIOGRAPHY

1. W.A. Wood, J. Sci. Inst. 18, 153 (1941).

2. W.A. Wood, Nature, London, 151, 585 (1943).

3. G.W. Brindley, Proc. Phys. Soc. 52, 117 (1940).

4. U. Dehlinger, Z. Krictallogr. 65, 615 (1927).
   W. Boas, Z. Kristallogr. 97, 354 (1937).

5. A.L. Patterson, Phys. Rev. 56, 972 (1939).

6. I. Waller, Nova. Acta. Roy. Soc. Sci. Upsal 11, 71 (1939).

7. A.R. Stokes and A.J.C. Wilson, Proc. Camb. Phil. Soc. 38, 313 (1942).
   A.R. Stokes and A.J.C. Wilson, Phys. Soc. Lond. 56, 1 74 (1943).

8. C.S. Smith and E.E. Stickley, Phys. Rev. 61, 191 (1943).

9. G.B. Greenough, Prog. Met. Phys. 3, (1952).

10. B.E. Warren, Prog. Met Phys. 8, 147 (1959).

11. A.R. Stokes, Proc. Phys. Soc. 61, 382 (1948).

12. B.E. Warren, Acta. Met. 11, 995 (1963).

13. J.B. Cohen and C.N.J. Wagner, Jour. of Appl. Phys. 33, 2073 (1962).

14. R.W. Hinton, L.H. Schwartz, and J.B. Cohen, Jour. Elchem. Soc. 110, 103 (1963).

15. O. Preston and N.J. Grant, Trans. Met. Soc. AIME 209, 371 (1957).

16. O. Preston and N.J. Grant, Trans. Mets Soc. AIME 221, 371 (1961).

17. N. Komatsu and N.J. Grant, Trans. Met. Soc. AIME 224, 705 (1962).

18. N.F. Mott and F.R.N. Nabarro, Conf. on Strength of Solids, Phys. Soc. Lond. (1948).

19. E. Orowan, Symposium on Internal Stresses in Metals and Alloys, Inst. of Met. Lond. 451 (1948).

20. J.C. Fisher, E.W. Hart, and R.H. Pry, Acta. Met. 1, 336 (1953).

21. W.S. Cremens and N.J. Grant, Proc. ASTM 58, (1958).

22. J. Weertman, NRL Rep. No. 5123, Nav. Resh. Lab. Wash, D.C. (1958).

23. J. Weertman and G.S. Ansell, Trans Met. Soc. AIME 147, 205 (1942).

24. Jens Rassemusen, ScD Thesis Massachusetts Institute of Technology (1963).

25. R.J. DeAngelis and L.H. Scheartz, Acta. Cryst. 16, 705 (1963).

26. L.H. Schwartz and J.B. Cohen, Amer. Cryst. Assoc. Mark I Computer Listing.

27. E.A. Faulkner, Phil. Mag. 5, 519 (1960).

28. M. Adachi and N.J. Grant, Trans. Met. Soc. 218, 881 (1960).

29. O.P. Agnihotri and G.B. Mitra, Phil. Mag. 8, (1963).

30. B.E. Warren and E.P. Warekois, Acta. Met. 3, 473 (1955).

31. C.N.J. Wagner, Acta. Met. 5, 427 (1957).

32. G.B. Greenough and E.M. Smith, Proc. Phys. Soc. B68, 51 (1955).

33. R.O. Williams, Acta. Met. 13, 163 (1965).

34. P. Gay, P.B. Hirsch, and A. Kelly, Acta. Cryst. 7, 41 (1954).

35. D. Mitchell and F.D. Haig, Phil. Mag. 2, 15 (1957).

36. H.G. Van Bueren, "Imperfections in Crystals," Interscience Publishers, Inc. New York (1960).

37. E. Gregory and N.J. Grant, Trans AIME. 200, 247 (1954).

38. B.L. Averbach, J.S. L. Leach, M.B. Beuer, and M.F. Comerford, Acta. Met. 4, 477 (1956).

39. C. Zener, Trans AIME 167, 550 (1946).

40. E.D. Hyam and J. Nutting, J. of Iron and Steel Inst. 184, 148 (1956).

41. L. Northcott, J. Inst. Metals 59, 225 (1936).

BIOGRAPHY

The author was born in 1940 in Franklin, Pennsylvania. He and his parents, Mr. and Mrs. C.S. Bridenbaugh Jr., moved to Bradenton, Florida where he received all of his elementary and secondary education.

He later received his Bachelor of Science degree in mechanical engineering in 1962 from Lehigh University. In 1963 he returned to Lehigh University to begin working towards a Master of Science degree in Metallurgical Engineering.

He is currently enrolled at Massachusetts Institute of Technology where he is a candidate for a Doctor of Philosophy in Metallurgy.